Astron. Astrophys. 280, 435–442 (1993)

ASTRONOMY AND ASTROPHYSICS

Selective gravitational microlensing and line profile variations in the BAL quasar H1413+117

D. Hutsemékers

Institut d'Astrophysique, Université de Liège, 5, av. de Cointe, B-4000 Liège, Belgium

Received February 22, accepted May 4, 1993

Abstract. In order to interpret the spectral differences observed between the four images of the gravitationally lensed broad absorption line (BAL) quasar H 1413+117, we have investigated the effect on the line profiles of the selective magnification of individual BAL clouds by gravitational microlenses.

Since microlenses magnify both the selected cloud and the whole BAL region, this effect is only differential, and general constraints on its capability to produce spectral variations have been derived.

Considering simple but realistic models for the microlenses, we find that the selective magnification of a relatively large optically thick BAL cloud can be at the origin of the spectral differences reported between the components of H 1413+117. However, a very precise configuration is needed: the magnified cloud must be at the border of the BAL region which must itself partially lie in a region of strong de-magnification. The fine tuning of the parameters necessary to reproduce the observations either seriously questions this kind of interpretation or puts strong constraints on the lensing models.

Another interpretation of the observed line profile differences in terms of effects due to microlensing is also briefly discussed.

Key words: gravitational lensing – BAL quasars – H 1413+117

1. Introduction

The quasar H 1413+117 was first recognised as a gravitational mirage by Magain et al. (1988). Due to the presence of a gravitational lens on the line of sight (most probably an undetected galaxy), the image of this quasar is splitted into four components of comparable brightness, which roughly form a square. As shown by Magain et al. (1988) and Angonin et al. (1990, hereafter A90), the spectra of the components are very similar, giving strong support to the lensing hypothesis.

Among the quasars presently known to the lensed, H 1413+117 is the only one to belong to the class of BAL quasars: in addition to emission lines, its spectrum displays large absorption troughs, blueshifted with respect to the emission, and usually interpreted in terms of mass outflows intrinsic to the quasar (see e.g. Weymann and Foltz 1983). H 1413+117 therefore provides us with a unique tool for studying simultaneously the gravitational lensing and BAL phenomena.

In the view, the effect of "microlenses" – i.e. individual stars generally belonging to the lensing galaxy (see e.g. Chang and Refsdal 1979, 1984; Schneider et al. 1992, hereafter S92) – is particularly interesting: with an effective lensing size comparable to the size of the continuum emitting region, they can magnify some parts of the BAL region located in front of the continuum, therefore revealing its structure.

Evidence for microlensing effects in H 1413+117 has been suggested by Kayser et al. (1990) on the basis of photometric variations of the component D, which is expected to show the strongest influence due to microlensing. Further evidence for microlensing effects in component D has been reported by A90. By obtaining spectra of the individual components with a bidimensional spectrograph, these authors found the normalized spectra of three of the components nearly identical while that of the component D is slightly different: the equivalent width of the emission lines is significantly smaller and the unsaturated part of the absorption profiles appears deeper (cf. Fig. 1). These characteristics are remarkably similar for the Si IV and C IV lines. It is important to notice that this behavior contrasts with the temporal variations detected in the spectra of some other BAL quasars, unrecognized to be lensed (see Barlow et al. 1992, and references therein). As done by A90, these spectral differences may be interpreted in terms of microlensing: if a stellar-like lens magnifies the

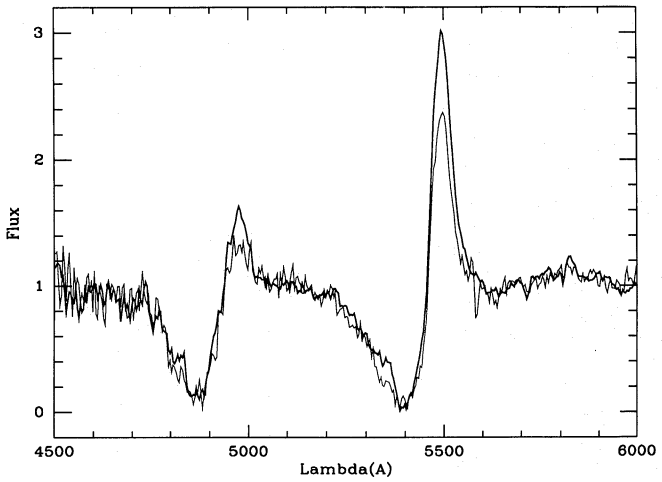

Fig. 1. The normalized spectrum of the component D of H 1413+117 (thin line) superimposed on the mean spectrum of the components A, B and C (thick line). The observations, obtained on March 7, 1989, are described in A90 and were kindly provided by the authors. The illustrated line profiles are those of Si IV and C IV. It should be noticed that the location of the continuum is not well defined especially between Si IV and C IV

continuum region but not the broad emission line region (BELR) which is much larger, the equivalent width of the emission lines decreases. This is a classical effect suspected to be at work in several gravitational lenses. However, after renormalization to the continuum, we expect no changes in the absorption profiles since these lines are formed just in front of the continuum emitting region [1]. There are at least two possibilities to explain in terms of microlensing the differences observed in the normalized absorption profiles: (1) the varying part of the absorption profile is filled in with emission (i.e. constituting a P Cygni type profile) and the variation of the absorption is in fact due to the apparent variation of the emission; (2) the absorption region consists of small clouds of different optical depth and the microlens selectively magnifies one (or a few) of them. This latter interpretation was discussed and favored by Surdej (1990) and A90. It is important to notice that the first interpretation requires a correlation between the variation in the normalized absorption profiles and the variation of the emission line equivalent widths, while in the second interpretation these variations may be uncorrelated, depending on the optical depth of the magnified cloud which may be optically thinner or thicker than the average. A distinction between these two interpretations, which clearly provide us with new insight on the BAL phenomenon itself, could be obtained by carrying out a regular spectral monitoring of H 1413+117.

The aim of the present paper is to investigate how quantitatively the selective magnification of BAL clouds can explain the spectral differences observed between the components of H 1413+117, considering simple but more realistic lens models than A90. A subsequent paper (Hutsemékers et al. 1993, hereafter Paper II) will be devoted to the study of microlensing effects on P Cygni type profiles (see also Hutsemékers et al. 1992).

In Sect. 2, we derive general constraints on the selective microlensing effect in the framework of a simple BAL cloud model. We apply these constraints in Sect. 3 and 4 to the case of H 1413+117, considering the Schwarzschild and Chang-Refsdal lens models. Discussion and conclusions form the last section.

2. The selective microlensing effect

Let us assume that the absorption at a given wavelength in a line profile is due to sub-regions of different optical depth (hereafter called clouds) and located in front of a continuum emitting region of radius R. The projected size of the whole BAL formation region evidently coincides with that of the continuum. In order to evaluate the selective amplification of the light coming from individual clouds, we isolate a cloud of radius r. The emergent line profile, normalized to the continuum, can be written:

$$f = (1-\varepsilon)\, e^{-\tau_\lambda} + \varepsilon\, e^{-\tau_\lambda^*} + e(\lambda), \qquad (1)$$

where τ_λ^* is the optical depth of the considered cloud, τ_λ the average optical depth of the other clouds and $e(\lambda)$ the emission line profile. $\varepsilon = r^2/R^2$ represents the size of the cloud at the considered wavelength.

If a microlens is located on the line of sight towards one of the quasar images, it magnifies both the whole BAL region and the selected cloud, with amplitudes determined by the radii and positions of these regions relative to the lens. For adequate combinations of radii and positions, the individual cloud may be *selectively magnified* relative to the remaining of the BAL region. In this model, the modified spectrum, normalized to the amplified continuum, is expressed by

$$f_* = \left(1 - \varepsilon \frac{A_*}{A}\right) e^{-\tau_\lambda} + \varepsilon \frac{A_*}{A}\, e^{-\tau_\lambda^*} + \frac{e(\lambda)}{A}, \qquad (2)$$

A_* and A respectively denoting the (de-)amplification factors for the selected cloud and for the whole BAL and continuum regions. These amplification factors are independent of λ, the gravitational lenses being achromatic. We also assume that the microlens has no effect on the emission lines, their region of formation being much larger than the continuum region. This approach differs from that of A90. Indeed, these authors have limited the influence of the lens

[1] It should be clear that, due to a microlensing effect, the attenuated continuum, i.e. the absorption lines, is (de-)amplified while the emission lines remain essentially unchanged. But, after renormalization to the adjacent continuum, also (de-)amplified, the normalized emission lines appear modified, while the normalized absorption profiles should be unchanged.

to its Einstein radius, neglecting its effect on the remaining part of the BAL region.

By comparing the normalized emission line profiles in the spectra with and without amplification, f_*^e and f^e respectively, the factor A can be easily derived:

$$A = \frac{f^e - 1}{f_*^e - 1}. \tag{3}$$

Now, if we consider the absorption profile at a wavelength where $e(\lambda) = 0$, we have from Eqs. (1) and (2)

$$f_*^a = (1-\beta)\, f^a + \beta\, e^{-\tau_\lambda^*}, \tag{4}$$

with

$$\beta = \frac{\varepsilon}{1-\varepsilon}\left(\frac{A_*}{A} - 1\right). \tag{5}$$

If β may be evaluated, Eq. (4) allows the derivation of τ_λ^* for an individual cloud. It is easy to imagine that if the lens is moving, a spectroscopic monitoring of the variations will provide us with a complete scan of the BAL region.

Because the selective magnification is in fact due to a differential effect between the individual cloud and the whole region, the amplitude of the possible profile variations may be severely constrained. Noting that we must always have $0 \leqq e^{-\tau_\lambda^*} \leqq 1$ and $0 \leqq e^{-\tau_\lambda} \leqq 1$, we obtain from Eqs. (1)–(5), the following upper limit on the relative profile variation $\Delta f = (f^a - f_*^a)/f^a$:

$$\Delta f \leqq \Delta f^m\,(\varepsilon, A, A_*) \tag{6}$$

where

$$\Delta f^m = \beta \qquad \text{if} \quad \varepsilon \leqq \varepsilon_L, \tag{7}$$

$$\Delta f^m = \beta\, \frac{1-\varepsilon}{\varepsilon}\, \frac{1-f^a}{f^a} \qquad \text{if} \quad \varepsilon \geqq \varepsilon_L, \tag{8}$$

and

$$\varepsilon_L = 1 - f^a. \tag{9}$$

These relations give an upper limit Δf^m on the amplitude of the absorption profile variations which may be induced by a selective microlensing effect. Lower limits may be derived similarly but are not considered here because the profile variations in H 1413+117 are characterized by $f_*^a \leqq f^a$. Let us notice that no observable variation may be expected for completely saturated profiles ($f_*^a = f^a = 0$).

In many situations of interest including those discussed in Sect. 3 and 4, Δf^m increases with ε for $\varepsilon \leqq \varepsilon_L$, while for $\varepsilon \geqq \varepsilon_L$, Δf^m decreases with ε. Consequently, for all ε we have

$$\Delta f^m \leqq \Delta f_L^m = \Delta f^m(\varepsilon_L, A, A_*). \tag{10}$$

Δf_L^m constitutes the upper limit on the amplitude of the possible variations independently of any hypothesis on the size and opacity of the clouds. These relations also indicate that there is an optimal size ε_L for an individual cloud to produce the largest possible profile variation. This optimal size does not depend on the amplification factors.

This behavior may be easily understood: if the cloud is very small, it may be strongly magnified compared to its surroundings but, smaller it is, less it contributes to the profile. Since the ratio A_*/A generally decreases with ε slower than $1/\varepsilon$, the largest differential magnification effect occur for the largest clouds, provided that $\varepsilon \leqq \varepsilon_L$ (cf. Eqs. (5)–(7)]. The minimum size for a cloud to produce an observable effect is therefore also fixed by Eq. (7). For example, if $\varepsilon \ll 1$, $A_*/A \sim \varepsilon^{-n/4}$, n being equal to 1, 2 or 4 (cf. the models discussed in the following sections), and we have $\Delta f^m \sim \varepsilon^{1-n/4}$, which, for $n = 2$ (Schwarzschild lens), simply reduces to $\Delta f^m \sim r/R$. This means that the largest possible relative profile variation due to the selective magnification of a very small absorbing cloud is of the order of magnitude of the cloud radius expressed in core radii.

The amplitude of the selective magnification effect on a BAL cloud depends not only on its size and on the ratio A_*/A, but also on the difference between the optical depths τ_λ^* and τ_λ. This difference must be as large as possible to produce the most noticeable effect, and, looking at Eq. (1), we can see that there is a limit when $\varepsilon = \varepsilon_L = 1 - f^a$, i.e. when $e^{-\tau_\lambda^*} = 0$ and $e^{-\tau_\lambda} = 1$. In this case, the BAL region consists of a single optically thick cloud of size ε_L, and the differential magnification effect is maximized.

In deriving Eq. (2), we have implicitely assumed that, except in the selected cloud, the optical depth of the whole BAL region is homogeneous. If the size of the clouds is sufficiently small, this approximation is reasonable, while, in other situations, it may be unrealistic. However, this approximation does not affect our analysis. Indeed, if the clouds in the vicinity of the considered one are optically thinner than the mean value (τ_λ), they will be more magnified than the average and the limits given in Eqs. (6)–(8) still constitute upper limits. If, on the contrary, the clouds in the vicinity of the selected one are optically thicker than the average, the effective size of the cloud, defined by its opacity, should be increased and the limits evaluated with a greater value of ε. It should be clear that what we call "cloud" in this paper is only a region of different optical depth seen in projection. It may have little to do with the clouds described in the models of Weymann et al. (1985), and Begelman et al. (1990), which are very small, most probably too small to be at the origin of detectable variations due to a selective magnification effect.

In the remaining sections, we will evaluate the theoretical limit Δf^m for some simple lens models in order to see if the variations detected in the absorption line profiles of

H 1413+117 may be explained by this selective magnification mechanism.

In the case of H 1413+117, we assume that the normalized, unmodified spectrum of the component D is identical to the average spectrum of the three other components. The spectra were divided according to Eq. (3), and A, the amplification factor of the whole BAL and continuum regions, estimated from the part of the C IV emission line profile where the signal-to-noise ratio is the highest i.e. where the intensity is greater than about 75% of the maximum intensity. On this part of the profile, the average values of A is equal to 1.45 ± 0.06. The uncertainty is due to the dispersion of the measurements on this part of the profile and from the uncertainty on the acceptable positions for the underlying continuum. We should notice that the values of A are not significantly different when estimated from the red side or from the blue side of this small part of the emission profile. The value derived from the center of the emission line may be slightly smaller, but it is not clear whether this is significant or not. In principle, the value of A may also be estimated from the Si IV line but it is much more dependent on the adopted underlying continuum while the signal-to-noise ratio is not as good as for C IV. In the limit of the uncertainties, the behavior of the Si IV line is nevertheless very similar to that of C IV (cf. Fig. 1).

The observed profile variation $\Delta f^{\rm obs}$ may be evaluated from the unsaturated part of C IV absorption line profile where the variations are detected and most noticeable ($\lambda \simeq 5350$ Å). In the wavelength range $\lambda\lambda$ 5330–5370 Å, the ratio $\Delta f^{\rm obs} = (f^a - f^a_*)/f^a$ is nearly constant and equal to 0.42 ± 0.06. As seen in Fig. 1, $f^a \sim 0.4$, so that $\varepsilon_L \sim 0.6$. If $\varepsilon = \varepsilon_L$, the BAL material absorbing in the wavelength range $\lambda\lambda$ 5350–5370 Å consists of a single optically thick cloud of size $\varepsilon_L = 0.6$. The absence of similar variations in the part of the profile immediately bluer suggests that, seen in projection, the BAL material absorbing at this wavelength is more homogeneous, as in the completely saturated, redder, part of the absorption profile. Such a cloud size should therefore be regarded with caution and, in the remaining, we will also consider the size $\varepsilon = 0.1$, less critical and still sufficiently large to produce a significant effect.

3. The Schwarzschild lens

Let us first assume that the continuum emitting region, the selected cloud and a Schwarzschild lens (point singularity) are centered on the line of sight. In this case, A and A_* have the well-known expressions (Liebes 1964; Refsdal 1964; S92):

$$A = \sqrt{1 + 4\frac{\eta_0^2}{R^2}} \quad \text{and} \quad A_* = \sqrt{1 + 4\frac{\eta_0^2}{r^2}}, \tag{11}$$

Table 1. Typical values of Δf_L^m computed for different combinations of ε_L and A

ε_L \ A	1.2	1.5	2.0	10.0	100.0
0.10	0.10	0.16	0.20	0.24	0.24
0.20	0.12	0.20	0.25	0.31	0.31
0.50	0.14	0.25	0.32	0.41	0.41
0.80	0.15	0.27	0.36	0.47	0.47
0.90	0.15	0.27	0.37	0.48	0.49

η_0 being the Einstein radius of the microlens projected in the source plane, i.e. $\eta_0^2 = 4GMc^{-2} D_{\rm s} D_{\rm ds} D_{\rm d}^{-1}$, where M is the mass of the lens, and $D_{\rm s}$, $D_{\rm d}$, $D_{\rm ds}$ are the angular diameter distances observer–source, observer–deflector and deflector–source, respectively (cf. S92). Combining these expressions, we immediately derive

$$A_* = \sqrt{1 + \frac{A^2 - 1}{\varepsilon}}. \tag{12}$$

This relation allows us to compute β and Δf_L^m as a function of ε_L and A. Typical values are given in Table 1. Since Δf_L^m represents the largest possible relative variation, we immediately see from that Table that the selective magnification effect is essentially a small effect. It is most noticeable for the largest values of A (i.e. of the global amplification of the continuum), and impossible if the continuum is not amplified itself ($A = 1$). It should be emphasized that Δf_L^m is not very dependent on small errors on A, and that, when A is large enough, Δf_L^m no longer depends on it.

For the particular case of H 1413+117, $A = 1.45 \pm 0.06$ and $\varepsilon_L = 0.6$ imply $\Delta f_L^m = 0.24 \pm 0.02$. For $\varepsilon = 0.1$, we have $\Delta f^m = 0.15 \pm 0.01$. These values are definitely smaller than $\Delta f^{\rm obs} = 0.42 \pm 0.06$. Even if we increase the value of A by typically $\sim 10\%$, this conclusion remains unchanged due to the small dependence on A of the amplitude of the selective magnification effect [2]. This means that the selective magnification effect due to a Schwarzschild-type lens cannot explain the profile differences observed in the component D of H 1413+117.

However, if we keep the lens centered on the selected cloud but not on the whole BAL region, we may hope to increase the effect. If D is the distance between the projected center of the lens and the center of the BAL/continuum region, the amplification approximately decreases as $1 - (d/2)^2$ provided that $d = D/R \leqq 1$ (Schneider and Wagoner 1987). Eq. (12) may therefore be generalized to

[2] For example, if the emission line profiles are partially affected by the microlens, the value of A estimated with Eq. (3) could be underestimated by typically 10% (see e.g. Schneider & Wambsganss 1990).

$$A_* = \sqrt{1 + \frac{A_c^2 - 1}{\varepsilon}} \tag{13}$$

where

$$A_c = A\left(1 - \frac{d^2}{4}\right)^{-1}. \tag{14}$$

In order to check the validity of this approximation, we have computed numerically the factor A_c for different values of d and η_0/R, and we found Eq. (14) to essentially constitute a good approximation. Adopting the largest possible value for d, $d = 1 - \sqrt{\varepsilon}$, we obtain $\Delta f_L^m = 0.27 \pm 0.02$ and $\Delta f^m(\varepsilon = 0.1) = 0.21 \pm 0.01$. Decentring the magnified cloud has clearly a negligible effect on the amplitude of the variations attributable to a selective magnification mechanism.

4. The Chang-Refsdal lens

If a point mass is located in a galaxy – a situation expected to occur frequently –, its gravitational potential may be perturbed by the galaxy and the resulting lens will considerably differ from the Schwarzschild model. This type of lens was first studied by Chang and Refsdal (1979, 1984) and we will refer to it as the Chang-Refsdal (CR) lens. A generic property of the CR lens amplification pattern is the presence of caustics or critical curves. When crossed by a light source, these curves are at the origin of strong magnification effects. In this situation, the amplification factors of the whole continuum region and the selected cloud may be approximated by the following expressions (cf. S92):

$$A = A_0 + \sqrt{\frac{g}{R}} \quad \text{and} \quad A_* = A_0 + \sqrt{\frac{g}{r}}, \tag{15}$$

which may be combined to give

$$A_* = A_0 + \frac{A - A_0}{\varepsilon^{1/4}}, \tag{16}$$

assuming both the cloud and the continuum simultaneously located on the critical curve. A_0 accounts for the underlying magnification related to other, distant sub-images, and g is a constant, roughly $\sim \eta_0$ (Chang 1984), which can be explicitely computed for a specific lens model.

It is now straightforward to estimate typical values of Δf^m in the case of H 1413+117. For $A_0 = 1$, $\Delta f_L^m = 0.06 \pm 0.01$ and $\Delta f^m(\varepsilon = 0.1) = 0.03 \pm 0.001$, while for $A_0 = 0$, $\Delta f_L^m = 0.20$ and $\Delta f^m(\varepsilon = 0.1) = 0.09$. We can see that these values strongly depends on A_0, but remain definetely too small to explain the spectra differences observed between the images of H 1413+117.

As in the Schwarzschild case, we may hope to increase the relative magnifications of the cloud and the whole BAL region by decentring the BAL region with respect to the caustic. For a CR lens, the dependence on the distance d is rather complex and asymmetric (Chang and Refsdal 1984; see also Fig. 6.13 in S92). Fortunately, since we are interested in the maximum effect, we can only consider the portion of the curve $-1 \leqq d \leqq 0$ where the gradient of the amplification is the largest. In this part of the curve, the variation of the amplification factor with d may be simply approximated by $1 - |d|$, such that Eq. (16) may be generalized to

$$A_* = A_0 + \frac{A - A_0}{(1 - |d|)\,\varepsilon^{1/4}}, \tag{17}$$

keeping the selected cloud on the caustic.

Adopting the largest possible distance, $|d| = 1 - \sqrt{\varepsilon}$, we find for $A_0 = 1$, $\Delta f_L^m = 0.22 \pm 0.02$ and $\Delta f^m(\varepsilon = 0.1) = 0.16 \pm 0.01$, while for $A_0 = 0$, $\Delta f_L^m = 0.70$ and $\Delta f^m(\varepsilon = 0.1) = 0.51$. These latter values are obviously greater than $\Delta f^{\text{obs}} = 0.42 \pm 0.06$. In this situation, the size ε of the smallest absorbing cloud which can be at the origin of the observed line variation is $\varepsilon \sim 0.04$ (i.e. $r/R \sim 0.2$).

We can therefore conclude that the spectral differences between the images of H 1413+117 may be explained by a selective magnification effect due to microlensing. However this effect requires a very precise lensing configuration: the caustic should be centered on the selected cloud while the remaining of the BAL region must be located in a region of strong de-magnification. Changing just a little bit the values of A_0 and d significantly reduces Δf^m. For example, adopting $A_0 = 0.3$, or adopting $A_0 = 0$ and $|d|$ smaller by only 10% lower $\Delta f^m(\varepsilon = 0.1)$ to the value of Δf^{obs}. Recalling also that the computed limits necessarily imply $e^{-\tau_\lambda^*} = 0$, we see that the interpretation in terms of selective magnification requires a fine tuning of the parameters.

Since the previous analytical approach is based on approximations which may affect these conclusions, it would be valuable to check the previous results with the help of numerical simulations. Such simulations will also allow us to investigate the selective magnification effect in the vicinity of singularities not considered analytically, like the behavior near cusps.

For this purpose, we may rewrite Eq. (7)

$$\frac{A_*(r)}{A(R,d)} \geqq 1 + \frac{1 - \varepsilon}{\varepsilon}\,\Delta f^{\text{obs}}, \tag{18}$$

which, for any $\varepsilon \leqq \varepsilon_L$, gives a lower limit on the ratio A_*/A needed to explain the observations. Adopting a value for ε, light curves for extended sources of radii R and $r = R\sqrt{\varepsilon}$ may be computed numerically for selected paths of the source through the amplification patterns produced by a CR lens model. Such light curves have been extensively

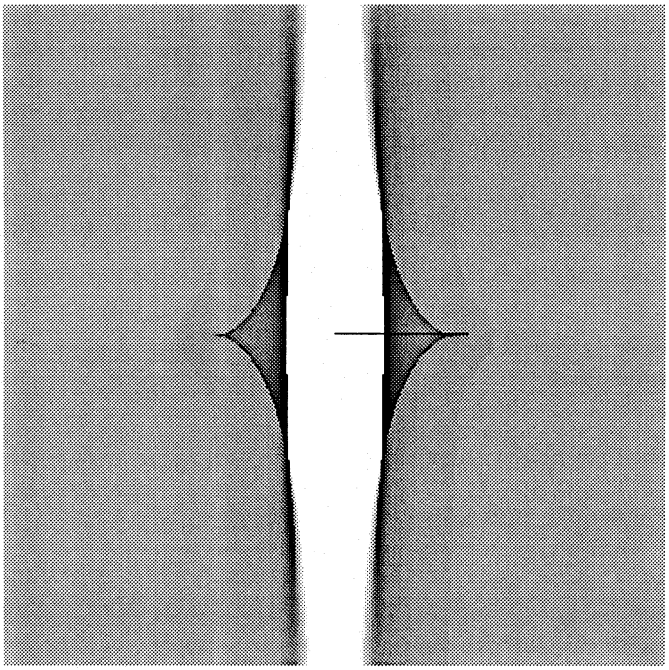

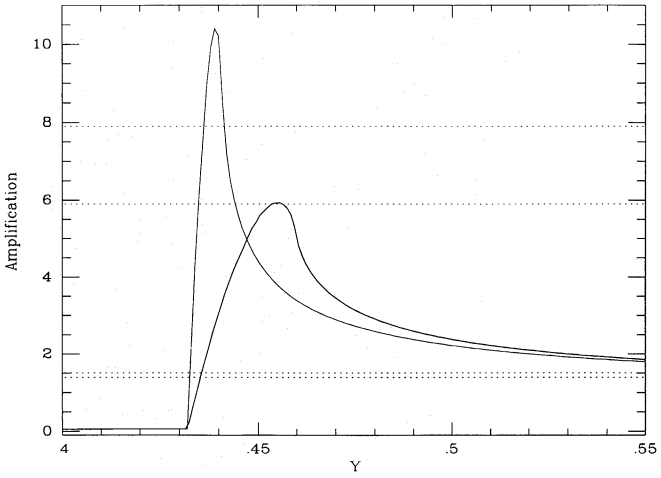

Fig. 2a and b. An example of a lensing configuration which can be at the origin of a selective magnification effect. **a** represents the amplification pattern in the source plane. A strong de-magnification region is present at the center (the darker the gray, the higher the amplification). The amplification factor has been normalized by the amplification due to the smoothed-out deflector. The shear γ and the normalized surface mass density κ_c are respectively equal to 1.1 and 0.0. The coordinates have been normalized following the relation $(Y_1, Y_2) = (\eta_1, \eta_2)/\eta_0 \sqrt{|1-\kappa_c+\gamma|}$ (the precise definition of all these quantities may be found in S92). In this figure, $-3 \leqq Y_1, Y_2 \leqq 3$. The path of the source is also drawn. **b** illustrates the values of $A_*(r)$ (thin line) and $A(R,d)$ (thick line) as a function of $Y = \sqrt{Y_1^2 + Y_2^2}$, for $\varepsilon = 0.1$ and $R/\eta_0 = 0.02$. The curve $A(R,d)$ was obtained by shifting the curve $A(R, d=0)$ by $\Delta Y = |d|\, R/\eta_0 \sqrt{|1-\kappa_c+\gamma|}$, where $|d| = 1-\sqrt{\varepsilon}$. The horizontal dashed lines indicate the limiting values for $A(R,d)$ and $A_*(r)$: 1.45 ± 0.06 and 6.9 ± 1.0, respectively. Near $Y \simeq 0.435$, both conditions $A(R,d) = 1.45 \pm 0.06$ and $A_*(r) \geqq 6.9 \pm 1.0$ simultaneously hold

discussed by many authors (see e.g. Kayser et al. 1986; S92). In this paper, the numerical integrations were performed in a standard way described with more details in Paper II. Let us only notice that we recover the curves presented by Grieger et al. (1989) for a single star CR lens.

In practice, we proceed as follows: by computing, for a given lens model, light curves in the vicinity of a singularity, we first estimate numerically the range of R values such that $A(R,d) = 1.45 \pm 0.06$, with $|d| \leqq 1-\sqrt{\varepsilon}$ being the distance from the singularity (point, fold, cusp, etc.). For example, when crossing a caustics, R should roughly range from $R_{\max}$ to $\varepsilon R_{\max}$, $R_{\max}$ being of the order of g/A^2 (cf. Eqs. (15), (17)). To the range of R values corresponds a series of values $r = R\sqrt{\varepsilon}$, for which it is easy to see if $A_*(r)$ satisfies Eq. (18). In the case of H 1413+117, and for $\varepsilon = 0.1$, $A_*(r)$ should be greater than 6.9 ± 1.0. By choosing R values and paths through to amplification patterns which largely encompass the allowed ranges of R and d, it is relatively easy, without too many simulations, to check if a given lensing configuration *cannot* provide us with the needed selective magnification effect. However, if a potentially interesting configuration is identified, the parameters must be further adjusted to verify that $A_*(r)$ can satisfy Eq. (18) simultaneously with $A(R,d) = 1.45 \pm 0.06$.

Simulations were performed for various CR lens models. They essentially confirms the previous conclusions: in order to have a significant effect, the selected BAL cloud must be at the border of the BAL region, centered on a high magnification region, while the remaining of the BAL/continuum region must be strongly de-magnified. For example, the typical diamond-shaped caustics, not associated to strong de-magnification regions, cannot provide us with the needed A_*/A ratio. Nor do the cusps, and this is not too surprising: despite being greater than that due to caustics, their magnification effect remains smaller than the magnification due to a Schwarzschild lens (Schneider & Weiss 1986), while they are more extended and not contiguous to a strong de-magnification region. An example of a lensing configuration able to selectively magnify a BAL cloud is illustrated in Fig. 2. Other possible configurations are those which produce overfucusing. In all cases, fine tuning of d and A_0 is required to have a sufficient effect.

5. Discussion and conclusions

In order to interpret the absorption line differences observed between the images of the gravitational mirage H 1413+117, A90 have suggested that absorbing clouds smaller than the continuum-forming region could be selectivelly magnified by a gravitational microlens. In this paper, we investigate further this effect, on the basis of more realistic microlens models.

From our study, we conclude that the selective magnification of an absorbing cloud by microlensing effects is possible but requires a very precise lensing configuration: the cloud must be located at the border of the projected continuum region, in a region of high magnification, while the remaining of the BAL region must suffer a strong de-magnification. The very fine tuning of the parameters which is needed to reproduce the observations may seriously question the plausibility of such a mechanism. However, if the profile differences may be actually attributed to this mechanism, this puts strong constraints on the lensing models for H 1413+117. Interestingly, the presence of a de-magnification region is compatible with the models proposed by Kayser et al. (1990) for H 1413+117, and more particularly with the first model which predicts the strongest dependence on microlensing for the component D ($\gamma \geqq 1$, cf. Fig. 2).

In the present paper, we have only considered single star models. However, the main results should not be very different for multiple star models, the amplification patterns still consisting of critical curves and points. Moreover, at large optical depths, multiple star models will certainly not favor the selective magnification since any differential effect will be smeared out. Even at moderate optical depths, the strong de-magnification regions of CR lens models tend to be "filled in" due to the influence of the distant stars (cf. Kayser et al. 1986).

The timescale of the variations may be roughly estimated. Adopting for the redshifts of the quasar and the deflector, $z_q = 2.55$ and $z_d = 1.55$, $H_0 = 75\,\mathrm{km\,s^{-1}\,Mpc^{-1}}$, $q_0 = 0$, the length scale η_0 may be evaluated: $\eta_0 \simeq 0.006$ pc, for a one solar mass star. Because the ratio of the distances of the quasar and the deflector is not very different from the unity, the transversal velocity V of the source relative to the microcaustics will not be strongly enhanced (cf. Kayser and Refsdal 1989). Therefore, adopting a few hundred of $\mathrm{km\,s^{-1}}$ for V, the characteristic microlensing timescale $\Delta t_0 = \eta_0 / V$ is of the order of 10 years.

To produce the low amplification $A = 1.45 \pm 0.06$ with the continuum region centered on the caustic ($A_0 = 0$), R is roughly equal to η_0, which is a reasonable value for the size of the continuum emitting region. This only constitutes an order of magnitude estimate of R, the exact value depending on the strength g of the caustic. If the caustic is decentered by $|d| = 1 - \sqrt{\varepsilon}$, the radius R is smaller by a factor ε and consequently, the timescale for the variations of the continuum, Δt_c, is $\sim \varepsilon \Delta t_0$, with a maximum amplification $A_{\max} \sim A/\sqrt{\varepsilon}$. The timescale for the absorption profile variations depends on the size of the cloud and may be estimated by $\Delta t_p \sim \sqrt{\varepsilon}\,\Delta t_c \sim \varepsilon \sqrt{\varepsilon}\,\Delta t_0$. Since only a small shift of the caustic may destroy the configuration needed for the selective magnification mechanism, Δt_p certainly constitutes an upper limit on the duration of the profile variation.

For a typical value $\varepsilon \simeq 0{,}1$, we have therefore $\Delta t_c \sim 1$ yr with $\Delta m_{\max} \sim 1\overset{m}{.}6$ and $\Delta t_p \sim 0.3$ yr. In the particular case illustrated in Fig. 2, we have $\Delta t_c \simeq 0.2$ yr, $\Delta m_{\max} \simeq 2\overset{m}{.}0$, and $\Delta t_p \simeq 0.06$ yr. The profile differences observed in component D of H 1413+117 should therefore be a relatively short-lived phenomenon if attributable to this mechanism. Let us also notice that on a timescale of 1 year, photometric variations larger than 1^m have not been reported for the component D of H 1413+117 (cf. A90). If the absence of such variations is confirmed, this may again seriously questions the plausibility of the selective magnification mechanism to explain the observed spectral differences.

If this kind of interpretation seems to have some difficulties to fit the observations, this does not mean that the absorption profile differences are not due to a microlensing effect. As discussed in Sect. 1, such differences may be attributed, at least qualitatively, to the apparent variation of an emission line superimposed on the absorption profile (see also Hutsemékers et al. 1992). Assuming that the underlying C IV absorption profile is completely saturated near $\lambda \simeq 5350$ Å, as it is near $\lambda \simeq 5400$ Å (see Fig. 1), we expect, near $\lambda \sim 5350$ Å, $f_* \simeq f/A \simeq 0.28 \pm 0.02$, a value which, in the limit of the uncertainties and without any other hypothesis, is in reasonably good agreement with the measured value. This kind of interpretation, which looks promising, will be discussed in more details in a subsequent paper. Let us finally recall that the profile differences may still be attributed to an intrinsic variation observed with a time delay between the different images of H 1413+117 (cf. A90).

Since a distinction between these interpretations, and therefore new understanding on the BAL phenomenon itself, may be obtained from regular observations, we cannot stress too much the importance of carrying out a spectroscopic monitoring of H 1413+117, as well as of other BAL quasars known to suffer spectral variations or located behind a galaxy (like 1E 0104+315, cf. Schneider & Weiss 1987).

Acknowledgements. It is a pleasure to thank Jean Surdej and Eddy Van Drom for a careful reading of the manuscript. We also thank Jean Surdej for providing us with the spectra published in A90. This research is supported in part by contract ARC 90/94-140 "Action de recherche concertée de la Communauté Française" (Belgium).

References

Angonin M. C., Remy M., Surdej J., Vanderriest C., 1990, A&A 233, L5 (A90)
Barlow T. A., Junkkarinen V. T., Burbidge E. M., Weymann R. J., Morris S. L., Korista K. T., 1992, ApJ 397, 81
Begelman M. C., de Kool M., Sikora M., 1991, ApJ 382, 416
Chang K., 1984, A&A 130, 157

Chang K., Refsdal S., 1979, Nature 282, 561
Chang K., Refsdal S., 1984, A&A 132, 168
Grieger B., Kayser R., Refsdal S., Stabell R., 1989, Abhandlungen auf der Hamburger Sternwarte X, 4, Hamburg
Hutsemékers D., Surdej J., Van Drom E., 1993, in preparation (Paper II)
Hutsemékers D., Surdej, Van Drom E., 1992, Gravitational lenses. Lecture Notes in Physics Vol. 406, Kayser R., Schramm T., Nieser L. (eds.), Springer, Berlin Heidelberg New York, p. 373
Kayser R., Refsdal S., 1989, Nature 338, 745
Kayser R., Refsdal S., Stabell R., 1986, A&A 166, 36
Kayser R., Surdej J., Condon J. J., Kellermann K. I., Magain P., Remy M., Smette A., 1990, ApJ 364, 15
Liebes S., 1964, Phys. Review 133, B835
Magain P., Surdej J., Swings J. P., Borgeest U., Kayser R., Kühr H., Refsdal S., Remy M., 1988, Nature 334, 327
Refsdal S., 1964, MNRAS 128, 294
Schneider P., Ehlers J., Falco E. E., 1992, Gravitational lenses, Springer, Berlin Heidelberg New York (S92)
Schneider P., Wagoner R. V., 1987, ApJ 314, 154
Schneider P., Wambsganss J., 1990, A&A 237, 42
Schneider P., Weiss R. V., 1986, A&A 164, 237
Schneider P., Weiss R. V., 1987, A&A 171, 49
Surdej J., 1990, Gravitational lensing. Lecture Notes in Physics Vol. 360, Mellier Y., Fort B., Soucail G. (eds.), Springer, Berlin Heidelberg New York, p. 57
Weymann R., Foltz C., 1983, Quasars and gravitational lenses, Swings J. P. (ed.), Liège Univ. Press, Liège, p. 538
Weymann R., Turnshek D. A., Christiansen W. A., 1985, Astrophysics of Active Galaxies and Quasi-Stellar Objects, Miller J. (ed.), Oxford Univ. Press, Oxford, p. 333